European Journal of Medicinal Chemistry 77 (2014) 176–184

Contents lists available at ScienceDirect

European Journal of Medicinal Chemistry

journal homepage: http://www.elsevier.com/locate/ejmech

Original article

QSAR on antiproliferative naphthoquinones based on a conformation-independent approach

Pablo R. Duchowicz [a,*], Daniel O. Bennardi [b], Daniel E. Bacelo [c], Evelyn L. Bonifazi [d], Carla Rios-Luci [e], José M. Padrón [e], Gerardo Burton [d], Rosana I. Misico [d,*]

[a] Instituto de Investigaciones Fisicoquímicas Teóricas y Aplicadas INIFTA (UNLP, CCT La Plata-CONICET), Diag. 113 y 64, C.C. 16, Sucursal 4, 1900 La Plata, Argentina
[b] Catedra de Química Organica, Facultad de Ciencias Agrarias y Forestales, Universidad Nacional de La Plata (UNLP), 60 y 119, B1904AAN La Plata, Argentina
[c] Departamento de Química, Facultad de Ciencias Exactas y Naturales, Universidad de Belgrano, Villanueva 1324, C1426BMJ Ciudad de Buenos Aires, Argentina
[d] Departamento de Química Orgánica y UMYMFOR (CONICET-UBA), Facultad de Ciencias Exactas y Naturales, Universidad de Buenos Aires, Pabellón 2, Ciudad Universitaria, C1428EGA Ciudad de Buenos Aires, Argentina
[e] BioLab, Instituto Universitario de Bio-Orgánica "Antonio González" (IUBO-AG), Centro de Investigaciones Biomédicas de Canarias (CIBICAN), Universidad de La Laguna, C/Astrofísico Francisco Sánchez 2, 38206 La Laguna, Spain

ARTICLE INFO

Article history:
Received 16 December 2013
Received in revised form
5 February 2014
Accepted 25 February 2014
Available online 26 February 2014

Keywords:
QSAR theory
Multivariable linear regression
Molecular descriptors
Cancer
Naphthoquinone derivative

ABSTRACT

The antiproliferative activities of a series of 36 naphthoquinone derivatives were subjected to a Quantitative Structure–Activity Relationships (QSAR) study. For this purpose a panel of four human cancer cell lines was used, namely HBL-100 (breast), HeLa (cervix), SW-1573 (non-small cell lung) and WiDr (colon). A conformation-independent representation of the chemical structure was established in order to avoid leading with the scarce experimental information on X-ray crystal structure of the drug interaction. The 1179 theoretical descriptors derived with E-Dragon and Recon software were simultaneously analyzed through linear regression models based on the Replacement Method variable subset selection technique. The established models were validated and tested through the use of external test sets of compounds, the Leave-One-Out Cross Validation method, Y-Randomization and Applicability Domain analysis.

1. Introduction

Quinones widely occurred in animals, plants and microorganisms, and often carried out indispensable roles in the biochemistry of energy production by providing vital links in the respiratory chain of living cells. These compounds acted as inhibitors of electron transport, uncouplers of oxidative phosphorylation, and gave rise to a wide range of cytostatic and antiproliferative activities [1]. Hence, quinones such as doxorubicin, salvicine, saframycin, saintopin, actinomycin D, etc. were widely used in cancer chemotherapy [2]. The National Cancer Institute (NCI) had identified the quinone unit as an important pharmacologic element for the cytotoxic activity, and it had been speculated that the latter was due to an intrinsic chemical property of the quinone core associated with other structural factors. Within the quinone group, the naphthoquinones (NQs) represented an important class of compounds with featured biological activities, where the 1,2- and 1,4-naphthoquinones had been considered privileged structures in Medicinal Chemistry [3–5].

Lapachol (**1**), a natural naphthoquinone, and many related heterocyclic derivatives, had been investigated during the past years mainly due to their antimicrobial [6,7], antifungal [8,9], trypanocidal [10], and anticancer activities [11]. β-Lapachone (**2**), a cyclization product of lapachol, had been demonstrated cytotoxic activity against a variety of cancer cells both *in vitro* and *in vivo*, and it was currently under phase II clinical trials as a new anticancer drug [12]. Although the cytotoxic action of β-lapachone had been known for more than 20 years [13], the detailed mechanism of action remained largely unknown.

It had been shown that the introduction of a hydroxyl group peri at the carbonyls of the 1,4-naphthoquinone nucleus increased its reduction potential by means of the formation of hydrogen bonds

* Corresponding authors.
E-mail addresses: pabloducho@gmail.com (P.R. Duchowicz), misicori@qo.fcen.uba.ar (R.I. Misico).

http://dx.doi.org/10.1016/j.ejmech.2014.02.057
0223-5234/

with the semiquinone radical and quinone dianion [14]. This effect might have been responsible for the enhancement in the biological activity of these NQs. There were few examples in the literature of natural or synthetic NQs with the characteristics above mentioned and all of them showed an enhanced antitumor activity as a direct consequence of the presence of such group [15–18].

In recent years, we had reported the synthesis and antiproliferative activities in human solid tumor cell lines of NQs related to lapachol and β-lapachone, with the goal of identifying new antitumor agents. Our main strategy was the introduction of hydroxy or methoxy groups on the benzene ring, resulting in 7-hydroxy-β-lapachone (**3**) as a lead with enhanced activity over the parent drug β-lapachone [19,20].

The well-known basis of the Quantitative Structure–Activity Relationships (QSAR) theory had been the hypothesis that the biological activity exhibited by a chemical compound was mainly determined by its molecular structure [21–23]. This fact did not offer specific details on the usually complex mechanism/path of the process that resulted in the final biological effect. However, it was possible to get some insight into the underlying mechanism of action by means of the QSAR-based predicted activities. Although naphthoquinones had been widely studied in the past in QSAR studies of their antiproliferative activities, many of such studies involved very few molecules [24–27], and others did not consider the simultaneous exploration of a great number of molecular descriptors for obtaining the best ones to be used in the QSAR model [28,29].

Among the main serious drawbacks that had suffered different widely used 3D-QSAR methods, such as Molecular Docking based QSAR [30], Comparative Molecular Field Analysis (CoMFA) [31] or Comparative Molecular Similarity Indices Analysis (CoMSIA) [32], the following ones were worth mentioning: i) the lack of accurate X-ray crystal structures showing the drug interaction, and ii) 3D-QSAR methods were not applicable to structurally diverse compound datasets [23]. In contrast, the conformation-independent 1D and 2D QSAR methods had been better suited for the development of relationships between the molecular structure and the biological activities of compounds [33].

In this work, we reported on the synthesis of a set of *ortho*-furanonaphthoquinones (**4**–**9**) with a hydroxyl group at position 6 or 9, and the evaluation of their antiproliferative activities against a panel of representative human solid tumor cell lines comprising HBL-100 (breast), HeLa (cervix), SW1573 (non-small cell lung), and WiDr (colon). We examined the experimental values of the antiproliferative activities observed for these compounds and the NQs previously synthesized by us (**1**–**3**, **10**–**36**), and developed a QSAR study to describe the structure-activity function. Herein, we described an approach that did not consider the conformational representation of the chemical structure by only relying on the constitutional and topological aspects of the molecules as previously argued [34] (Fig. 1).

2. Results and discussion

2.1. Chemistry

Compounds **1**–**3** and **10**–**36** were prepared according to previously reported in-house methods [19,20]. The hydroxydunniones (**4**–**7**) were obtained from 5-hydroxydunniol (**32**) and 8-hydroxydunniol (**33**) under different acidic conditions as shown in Scheme 1. Thus, treatment of **32** with methanesulfonic acid gave selectively compound **4** while reaction of the latter with 20% hydrochloric acid under reflux gave **37**. Compound **6** was obtained in 15% yield upon reaction of **37** with concentrated sulfuric acid overnight (compound **37** was recovered in 74% yield).

In a similar way, treatment of 8-hydroxydunniol (**33**) with methanesulfonic acid gave quantitatively compound **5**. Isomerization of the latter compound required harsher conditions than those used above, treatment with concentrated hydrochloric acid at 85 °C overnight gave **38** in 50% yield (39% of unreacted **5** was recovered).

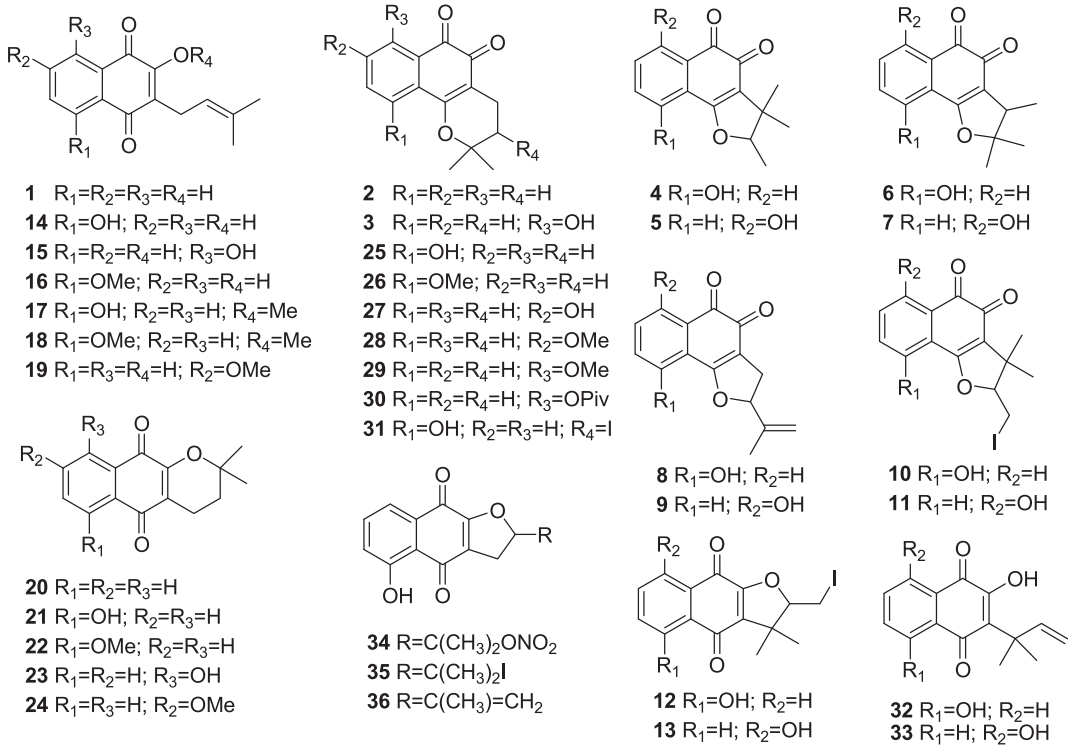

Fig. 1. Structures of naphthoquinones analyzed.

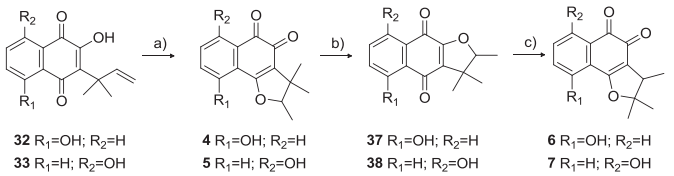

Scheme 1. Synthesis of hydroxydunniones **4**–**7**. *Reagents and conditions*: a) MsOH; b) HCl; c) H_2SO_4 (c).

Compound **7** was obtained in 32% yield upon reaction of **38** with concentrated sulfuric acid (55% of unreacted **38** was recovered). Attempts to carry out the isomerization of compounds **4** and **5** to **6** and **7**, respectively with concentrated sulfuric acid were unsuccessful.

Due to the interesting antiproliferative activity exhibited by 5-hydroxy-dehydro-*iso*-α-lapachone (**36**) [17] we decided to carry out the synthesis and antiproliferative evaluation of the isomeric orthoquinone **8**. Thus, 5-hydroxylapachol (**14**) was reduced with zinc and acetylated *in situ* to give the intermediate peracetylated hydroquinone (not isolated) that was immediately oxidized with selenium dioxide (Scheme 2). Subsequent deacetylation gave 5-hydroxylomatiol (**39**). Compound **8** was obtained in 50% overall yield by cyclization of **39** with aqueous sulfuric acid at low temperature and short reaction time. Using the same reaction sequence, compound **9** was obtained in 54% overall yield from 8-hydroxylapachol (**15**) (Scheme 2).

2.2. Biology

2.2.1. Antiproliferative activity of the synthesized compounds

The naphthoquinones **1**–**36** were screened for their antiproliferative effects on a panel of human solid tumor cells: HBL-100 (breast), HeLa (cervix), SW1573 (non-small cell lung), and WiDr (colon) and the results, expressed as GI_{50}, were obtained using the SRB assay [35]. Table 1 shows the antiproliferative activities of all the naphthoquinones assayed in the QSAR study. The experimental antiproliferative potencies were converted into logarithm $pGI_{50} = -\log_{10}GI_{50}$, for the QSAR study. The variation range of the activities in each human solid tumor cell line was: HBL-100 (breast) [−1.4914, 1.4437], HeLa (cervix) [−2.0000, 0.6778], SW-1573 (non-small cell lung) [−2.0000, 1.5376], and WiDr (colon) [−2.0000, −0.2553].

Direct comparison between *para* and *ortho* tricyclic isomers showed comparable activity for furanonaphthoquinones, while in the case of pyranonaphthoquinones generally the β isomer was more active than the α. Comparison between *o*-furanonaphthoquinones with a hydroxyl group at position 6 or 9 of the aromatic ring showed that the presence of a *peri* hydroxyl increased antiproliferative activity in some cell lines, while for other lines the activity was comparable. Compound **3** gave the best results of all the evaluated NQs in three of the tested cell lines, being 29 times more active than β-lapachone on SW1573 cells.

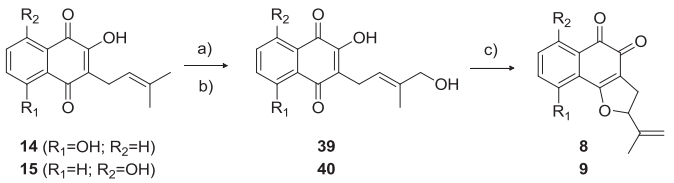

Scheme 2. Synthesis of compounds **8** and **9**. *Reagents and conditions*: a) Zn, Ac_2O, Et_3N, rt, b) *i*. SeO_2, Ac_2O, HAcO, 150 °C, *ii*. MeOH, KOH 6 M, reflux; c) H_2SO_4:H_2O (5:3), 0 °C.

Table 1
GI_{50} values of naphthoquinones against human solid tumor cells.[a]

Compound	HBL-100 (breast)	HeLa (cervix)	SW1573 (lung)	WiDr (colon)
1[b]	7.8 (±4.6)	2.3 (±0.8)	34 (±6.5)	36 (±9.8)
2[b]	0.38 (±0.14)	1.0 (±0.4)	0.84 (±0.32)	2.0 (±0.2)
3[c]	0.036 (±0.009)	0.21 (±0.04)	0.029 (±0.007)	2.0 (±0.2)
4	2.2 (±0.1)	1.9 (±0.1)	2.4 (±0.2)	19 (±1.1)
5	0.54 (±0.11)	1.9 (±0.1)	0.99 (±0.05)	5.2 (±1.3)
6	2.0 (±0.1)	0.90 (±0.03)	1.3 (±0.1)	2.1 (±0.7)
7	0.34 (±0.01)	1.80 (±0.07)	0.48 (±0.03)	16 (±5.3)
8	3.0 (±0.2)	3.0 (±0.2)	2.70 (±0.01)	26 (±2)
9	0.46 (±0.05)	0.21 (±0.01)	1.00 (±0.02)	2.2 (±0.3)
10	1.8 (±0.1)	1.6 (±0.3)	1.6 (±0.2)	1.8 (±0.1)
11	0.46 (±0.02)	1.5 (±0.3)	0.80 (±0.29)	1.9 (±0.1)
12[b]	1.9 (±0.3)	1.7 (±0.4)	1.3 (±0.3)	2.0 (±0.03)
13[b]	0.41 (±0.05)	1.3 (±0.3)	0.40 (±0.13)	2.0 (±0.2)
14[b]	0.60 (±0.12)	0.42 (±0.11)	0.70 (±0.23)	6.3 (±1.9)
15[b]	21 (±4.1)	2.6 (±0.4)	18 (±2.7)	19 (±2.4)
16[c]	22 (±2.9)	30 (±13)	26 (±4.5)	>100
17[b]	20 (±6.9)	3.5 (±0.6)	4.8 (±0.2)	20 (±2.7)
18[b]	17 (±2.3)	18 (±1)	5.8 (±1.7)	28 (±5.5)
19[c]	19 (±0.6)	18 (±0.8)	17 (±2.0)	68 (±16)
20[b]	14 (±4.5)	15 (±2.6)	3.1 (±0.1)	26 (±0.6)
21[b]	2.6 (±0.8)	12 (±1.2)	2.7 (±0.7)	18 (±1.6)
22[c]	28 (±3.1)	>100	>100	>100
23[c]	3.4 (±0.2)	1.8 (±0.2)	19 (±0.9)	14 (±2.2)
24[c]	28 (±4.1)	40 (±8.6)	27 (±3.0)	82 (±13)
25[c]	0.62 (±0.16)	1.1 (±0.2)	0.36 (±0.01)	1.9 (±0.1)
26[c]	0.69 (±0.03)	1.8 (±0.4)	0.46 (±0.01)	2.1 (±0.2)
27[c]	2.3 (±0.1)	2.5 (±0.3)	2.3 (±0.1)	21 (±1.6)
28[c]	0.41 (±0.16)	1.7 (±0.2)	0.45 (±0.15)	27 (±0.8)
29[c]	2.7 (±0.4)	5.1 (±0.4)	1.4 (±0.5)	86 (±25)
30[c]	0.18 (±0.05)	1.6 (±0.03)	0.23 (±0.01)	2.1 (±0.03)
31[b]	1.1 (±0.1)	1.3 (±0.4)	0.56 (±0.01)	1.9 (±0.1)
32[b]	31 (±3)	28 (±1.6)	36 (±6.3)	31 (±1.6)
33[b]	16 (±1.8)	24 (±5.3)	3.8 (±1.3)	23 (±1.8)
34[b]	2.8 (±0.5)	2.2 (±0.34)	2.8 (±1.3)	18 (±2.1)
35[b]	0.94 (±0.36)	0.8 (±0.41)	0.83 (±0.35)	2.0 (±0.1)
36[b]	2.0 (±0.5)	2.4 (±0.7)	2.3 (±0.5)	1.9 (±0.2)

[a] Values are given in μM and are means of three to six experiments (±standard deviation).
[b] Data from *Bioorg. Med. Chem.* 18 (2010), 2621–2630.
[c] Data from *Eur. J. Med. Chem.* 53, 2012, 264–274.

2.3. Model development

2.3.1. Molecular descriptors selection in MLR

In recent years, theoretical and experimental researchers had focused an increasing attention on finding the most efficient tools for selecting molecular descriptors in QSAR studies. There were available a great number of feature selection methods to search for the best descriptors from a pool of variables, and the Replacement Method (RM) [36,37], employed here, had been successfully applied elsewhere [38–42]. In brief, the RM was an efficient optimization tool which generated Multivariable Linear Regression (MLR) based models on the training set by searching in a set having D descriptors for an optimal subset having $d << D$ ones with smallest training set standard deviation (S_{train}) or smallest root mean square deviation ($RMSD_{train}$). Table 1S included a list of mathematical equations used in the present study, with definitions for S and RMSD. The quality of the results achieved with this technique approached that obtained by performing an exact (combinatorial) full search of molecular descriptors although, of course, required much less computational work. However, in some cases, the RM could get trapped in a local minimum of S. Although such local minima provided acceptable models, an improvement of the method had been developed in the Enhanced Replacement Method (ERM) [43,44]. The Matlab 7.12 software was used in all our calculations [45].

2.3.2. Model validation

The most efficient validation strategy had always consisted on using an external test set of molecules, never seen by the model during the calibration of its parameter values. For this purpose, the training set included 30 naphthoquinone derivatives and the test set the remaining 6 compounds. This partition was chosen for each human solid tumor cell line in such a way that both sets shared similar qualitative structure-activity characteristics, as the training set should be representative of the molecular diversity of all the compounds under study and uniformly span over the whole activity range.

The Cross-Validation technique of Leave-One-Out (loo) was practiced [46]. The parameters R^2_{loo} and S_{loo} (square of the correlation coefficient and standard deviation of Leave-One-Out) measured the stability of the model upon exclusion of molecules. According to the literature, R^2_{loo} should be greater than 0.5 for a validated model.

The Y-Randomization procedure [47] was also applied in order to verify that the model was robust. This technique consisted on scrambling the experimental property values in such a way that they did not correspond to the respective compounds. After analyzing 50,000 cases of Y-Randomization, the standard deviation obtained (S^{rand}) had to be a poorer value than the one found by considering the true calibration (S).

2.3.3. Applicability domain analysis

The applicability domain (AD) for the QSAR models was also explored, as not even a predictive model was expected to reliably predict the modeled activity for the whole universe of molecules. The AD was a theoretically defined area that depended on the descriptors and the experimental activity [48]. Only the molecules falling within this AD were not considered model extrapolations. One possible way to characterize the AD was based on the leverage approach [49], which allowed to verify whether a new compound could be considered as interpolated (with reduced uncertainty, reliable prediction) or extrapolated outside the domain (unreliable prediction). Each compound i had a calculated leverage value (h_i) and there existed a warning leverage value (h^*); Table 1S included the definitions for h_i and h^*. When $h_i > h^*$ for a test set compound, then a warning should be given: it meant that the prediction was the result of substantial extrapolation of the model and could not be treated as reliable.

2.3.4. Degree of contribution for a descriptor

In order to find out the relative importance of the j-th descriptor in the linear model, the regression coefficients (b^s_j, see Table 1S) were standardized. The larger was the absolute value of b^s_j, the greater was the importance of such descriptor [50].

2.3.5. Discussion of QSAR results

The most representative structural features of the training set of 30 naphthoquinones were identified in the panel of four human solid tumor cell lines, by applying the RM technique for searching the best 1–4 descriptor linear regressions. We followed the common practice of keeping the model's size as small as possible, in order to avoid any possible fortuitous correlation. According to this, we chose structure–activity relationships having 3-descriptors with an acceptable predictive power on the test set. The best MLR found were listed in Table 2S, while a brief description of the involved descriptors was provided in Table 3S. It was appreciated from Table 2S that the $RMSD_{train}$ parameter continued improving beyond such number of 3 variables, but $RMSD_{test}$ did not improve. The following models were established:

HBL-100:

$$pGI_{50} = -1.502ICR - 3.860GATS5e - 2.742BELe7 + 8.640 \quad (1)$$

$$R^2_{train} = 0.68,\ S_{train} = 0.44,\ R^2_{ij\ max} = 0.19,\ o(2.5S) = 0$$

$$R^2_{loo} = 0.55,\ S_{loo} = 0.52,\ S^{rand} = 0.51,\ R^2_{test} = 0.80,\ S_{test} = 0.58$$

HeLa:

$$pGI_{50} = -4.684GATS5e - 57.240JGI6 - 0.840O - 060 + 6.057 \quad (2)$$

$$R^2_{train} = 0.67,\ S_{train} = 0.38,\ R^2_{ij\ max} = 0.50,\ o(2.5S) = 0$$

$$R^2_{loo} = 0.56,\ S_{loo} = 0.44,\ S^{rand} = 0.41,\ R^2_{test} = 0.78,\ S_{test} = 0.46$$

SW-1573:

$$pGI_{50} = -7.216EEig11x + 10.046EEig11r - 7.883BELp7 + 8.666 \quad (3)$$

$$R^2_{train} = 0.73,\ S_{train} = 0.42,\ R^2_{ij\ max} = 0.91,\ o(2.5S) = 0$$

$$R^2_{loo} = 0.65,\ S_{loo} = 0.48,\ S^{rand} = 0.48,\ R^2_{test} = 0.86,\ S_{test} = 0.45$$

WiDr:

$$pGI_{50} = -1.939ICR + 2.336\,ATS6v - 4.715\,BELe7 - 0.158 \quad (4)$$

$$R^2_{train} = 0.76,\ S_{train} = 0.32,\ R^2_{ij\ max} = 0.31,\ o(2S) = 0$$

$$R^2_{loo} = 0.68,\ S_{loo} = 0.37,\ S^{rand} = 0.40,\ R^2_{test} = 0.96,\ S_{test} = 0.23$$

here, R_{ijmax} denoted the maximum correlation coefficient between descriptor pairs, $o(2S)$ indicated the number of outlier compounds having a residual (difference between experimental and calculated activity) greater than 2 times S_{train} and lower than three times S_{train}.

Equations (1)–(4) had an acceptable predictive power on the external test sets including each one 6 naphthoquinone compounds, according to R^2_{test} and S_{test} parameters. Such models approved the internal validation process of Cross-Validation through the exclusion of one molecule at a time. The Y-Randomization technique demonstrated that all these equations had $S_{train} < S^{rand}$ and thus valid structure–activity relationships were achieved. We checked that these equations accomplished with the external validation criteria recommended in Ref. [46] to assure predictive capability, that was to say:

- $1 - R^2_0/R^2_{test} < 0.1$ or $1 - R'^2_0/R^2_{test} < 0.1$
- $0.85 \le k \le 1.15$ or $0.85 \le k' \le 1.15$
- $R^2_m > 0.5$

The R^2_0, R'^2_0, k, k' and R^2_m parameters appeared defined in Table 1S and were presented in Table 4S for each model.

Fig. 2 plotted the predicted antiproliferative pGI_{50} activities as function of the experimental values for the training and test sets (numerical data were provided in Table 5S), showing that there existed a tendency for the points to have a straight line trend in

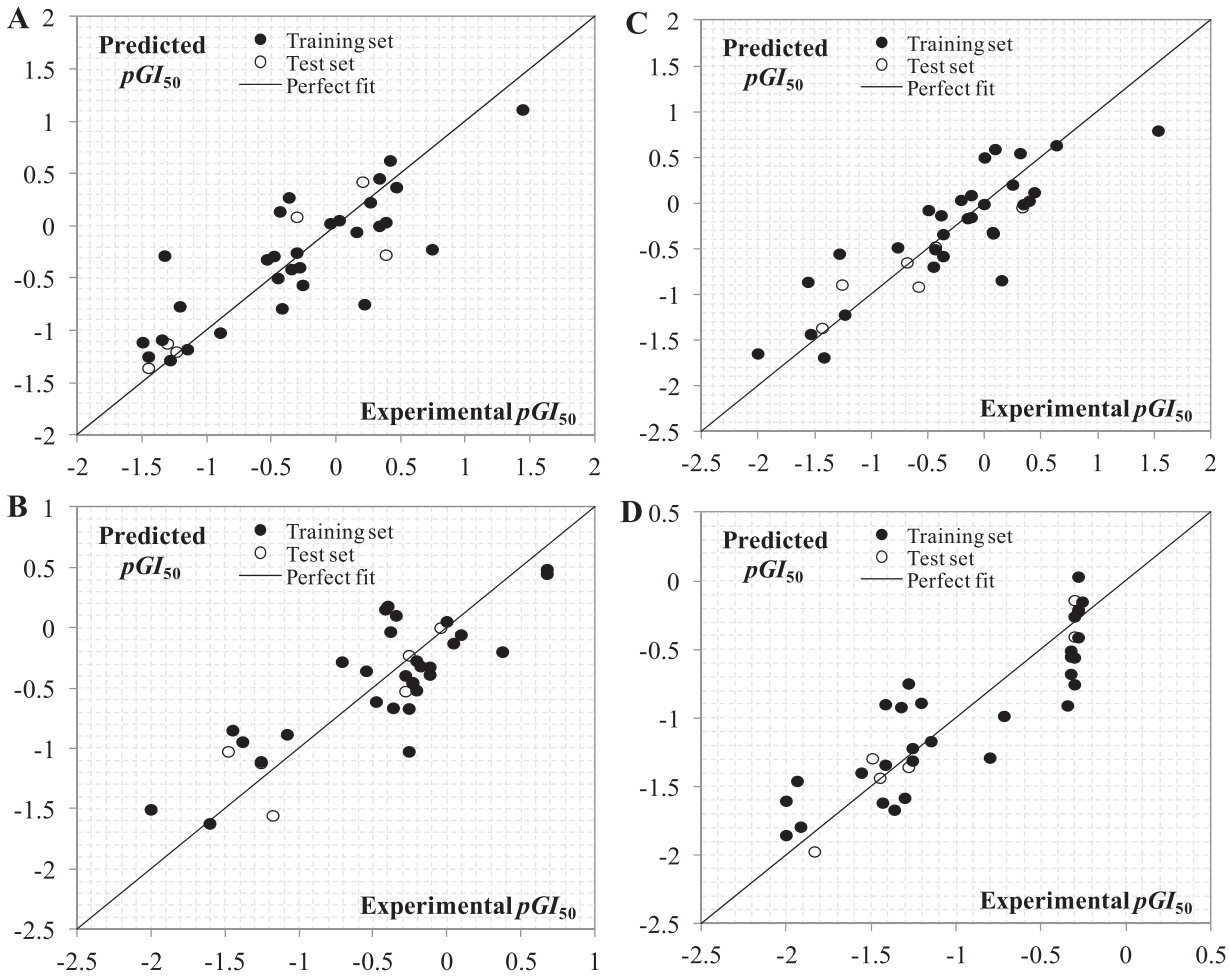

Fig. 2. Predicted antiproliferative activities as a function of experimental values for A. HBL-100; B. HeLa; C. SW-1573; D. WiDr.

each cell line. The dispersion plots of residuals (i.e. residuals as a function of predicted activities) in Fig. 1S revealed that residuals tended to obey a random pattern around the zero line, suggesting that the assumption of the MLR technique was fulfilled. The correlation matrices of Eqs. (1)–(4) were given in Table 6S, and showed the absence of very high correlations between descriptors pairs. The numerical values taken by the molecular descriptors were included in Table 7S.

The conformation-independent descriptors appearing in Eqs. (1)–(4) belonged to five different families [51]: i) Topological: *ICR*, radial centric information index; ii) 2D-Autocorrelation: *GATS5e*, Geary autocorrelation of lag 5 weighted by Sanderson electronegativity; *ATS6v*, Broto-Moreau autocorrelation of lag 6 (log function) weighted by van der Waals volume; *JGI6*, mean topological charge index of order 6; iii) BCUT: *BELe7*, lowest eigenvalue 7 of Burden matrix weighted by Sanderson electronegativity; *BELp7*, lowest eigenvalue *n*. 7 of Burden matrix weighted by atomic polarizability; iv) Edge Adjacency Index: *EEig11x*, eigenvalue 11 from Edge Adjacency matrix weighted by edge degree; *EEig11r*, eigenvalue 11 from Edge Adjacency matrix weighted by resonance integral; v) Atom Centred Fragment: *O-060*, number of Al–O–Ar/Ar–O–Ar/R…O…R/R–O–C = X groups. In addition, none of these descriptors were of the TAE type.

The relative importance of the molecular descriptors involved in Eqs. (1)–(4) was presented in Table 2. For instance, in Eq. (1) the absolute standardized regression coefficient had a greater value for *GATS5e* (0.69) when compared to *ICR* (0.36) and *BELe7* (0.28). This meant that *GATS5e* contributed more than the rest of the variables to the numerical variation of the activity in the training set, and this was the main reason why this specific descriptor was selected during the application of the RM approach.

As every molecular descriptor in Eqs. (1)–(4) took positive numerical values (Table 7S), it was concluded that positive regression coefficients made the associated descriptors to have a positive contribution on the predicted potencies, while negative coefficients made the descriptors to have a negative contribution on the predictions. Therefore, the higher were the positive contributions in the equations (also considering the sign of the constant), then the greater was the tendency on the predicted pGI_{50} activity to have a high value in a naphthoquinone derivative. Of course, as the established models were statistical in nature, a highly negative predicted activity meant for instance that it was quite probable for the compound to display a poor potency.

Table 2
Relative importance of the molecular descriptors of Eqs. (1)–(4). The absolute standardized regression coefficients are given in parentheses.

Eq. (1)	*ICR* (0.36)	*GATS5e* (0.69)	*BELe7* (0.28)
Eq. (2)	*GATS5e* (0.96)	*JGI6* (0.46)	*O-060* (0.58)
Eq. (3)	*EEig11x* (1.27)	*EEig11r* (2.09)	*BELp7* (0.88)
Eq. (4)	*ICR* (0.52)	*ATS6v* (0.80)	*BELe7* (0.63)

The analysis of the applicability domains of Eqs. (1)–(4) revealed that all the compounds included in the test sets of each cell line belonged to the AD of the models ($h_i < h^*$). Thus, the predicted anticancer activities for such naphthoquinones were considered as reliable. The leverage values were provided in Table 8S.

Finally, an alternative validation of the established QSAR was performed. It was corroborated what happened when these structure–activity relationships were exposed to independent data, e.g. put the antiproliferative activity of HBL-100 into the SW-1573 model and vice versa. The results found were provided in Table 3. According to the S_{train} and S_{test} parameters, it was seen that Eqs. (1)–(4) were specific to the cell line for which they were calibrated, as the statistical parameters deteriorated the models when applied on other data. Therefore, the herein established QSAR were able to discriminate in the tumor cell panel.

3. Conclusions

The search of new antitumor agents had been considered of main interest in the Medicinal Chemistry field. In this work, the relationships between the chemical structures of new hydroxynaphthoquinone derivatives to their antiproliferative potencies were investigated. The established linear models were specific to the each cancer cell line and had an acceptable predictive performance on the test sets, and were able to fulfill other necessary mathematical conditions, such as Cross-Validation, Y-Randomization and Applicability Domain analysis. Finally, the contributions of molecular descriptors were discussed, in order to elucidate the structural characteristics for a naphthoquinone derivative to exhibit a favorable potency. For instance, when the molecular structures leaded to high positive contribution of descriptors in the QSAR equations, then the greater was the tendency on the predicted activity to have a high value in a naphthoquinone derivative.

The use of the conformational representation of the chemical structure was avoided, and thus no-experimental information on X-ray crystal structure of the drug interaction was required. From the computational point of view, the exclusion of 3D structural aspects also avoided problems associated with ambiguities that resulted from an incorrect geometry optimization due to the existence of compounds in various conformational states. Such kind of problems would also have leaded to the loose of predictive capability of the QSAR. Some of us had been working in the use of new methods based on constitutional or topological approximations to QSAR studies and new results would be published shortly elsewhere.

4. Experimental section

4.1. General

Melting points were taken on a Fisher-Johns apparatus and are uncorrected. IR spectra were recorded in thin films using KBr disks on a Nicolet Magna 550 FT-IR spectrophotometer, values were given in cm^{-1}. ^1H and ^{13}C NMR spectra were recorded on a Bruker Avance II 500 spectrometer at 500.13 and 125.77 MHz respectively, in deuterochloroform unless indicated otherwise. Chemical shifts were given in ppm downfield from TMS as internal standard, J values are given in Hz. Multiplicity determinations and 2D spectra (COSY, HSQC and HMBC) were obtained using standard Bruker software. High-resolution mass spectra (HRMS) were measured on an Agilent LCTOF, high resolution TOF analyzer or a Bruker micrOTOF-Q II spectrometer with ESI ionization in positive mode. Reactions were monitored using thin-layer chromatography (TLC) on aluminum backed precoated Silica Gel 60 F254 plates (E Merck). In general, naphthoquinones were highly colored and were visible on a TLC plate; colorless compounds were detected using UV light. Flash chromatography was carried out using silica gel 60 (230–400 mesh) with the solvent system indicated in the individual procedures. All solvent ratios were quoted as v/v. Solvents were evaporated at reduced pressure and ca. 45 °C.

Table 3
Comparison of specificity of developed QSAR models on different human cancer cell lines. The selected results are shown in bold.

	Eq. 1	Eq. 2	Eq. 3	Eq. 4
HBL-100	$S_{train} = 0.44$ $S_{test} = 0.58$	$S_{train} = 0.53$ $S_{test} = 0.83$	$S_{train} = 0.45$ $S_{test} = 0.87$	$S_{train} = 0.54$ $S_{test} = 1.21$
HeLa	$S_{train} = 0.42$ $S_{test} = 0.49$	$S_{train} = 0.38$ $S_{test} = 0.46$	$S_{train} = 0.44$ $S_{test} = 1.27$	$S_{train} = 0.50$ $S_{test} = 0.65$
SW-1573	$S_{train} = 0.49$ $S_{test} = 0.88$	$S_{train} = 0.54$ $S_{test} = 1.30$	$S_{train} = 0.42$ $S_{test} = 0.45$	$S_{train} = 0.61$ $S_{test} = 0.57$
WiDr	$S_{train} = 0.48$ $S_{test} = 0.53$	$S_{train} = 0.53$ $S_{test} = 0.74$	$S_{train} = 0.42$ $S_{test} = 0.38$	$S_{train} = 0.32$ $S_{test} = 0.23$

4.2. Chemistry

Lapachol (**1**) was extracted from the powdered wood of *Tabebuia impetiginosa* (Bignoniaceae) and was purified by a series of recrystallizations [52]. From this quinone, α-lapachone (3,4-dihydro-2,2-dimethyl-2H-benzo-[*g*]chromene-5,10-dione, **20**) and β-lapachone (3,4-dihydro-2,2-dimethyl-2H-benzo[h]chromene-5,6-dione, **2**) were obtained by intramolecular cyclization using concentrated hydrochloric acid and concentrated sulfuric acid, respectively [53].

Compounds **14** and **32** were obtained from 2-hydroxy-1,4-naphthoquinone. In a similar way, **15** and **33** were synthesized from 3-hydroxy-1,4-naphthoquinone. Treatment of 5-hydroxylapachol (**14**) with dimethyl sulfate lead to compounds **17** and **18**. The cyclization of **14** with CAN gave naphthoquinones **34** and **35**. The addition of iodine to compounds **14**, **32**, and **33** gave the iodinated naphthoquinones **10**–**13**, **31** and **36** as described previously.

5-Methoxylapachol (**16**) and 7-methoxylapachol (**19**) were prepared from commercially available 5-methoxytetralone and 7-methoxytetralone (Sigma–Aldrich), respectively. The pyranonaphthoquinones **21**/**25**, **3**/**23**, **22**/**26** and **28**/**24** were obtained by cyclization under acidic conditions of lapachol derivatives **14**, **15**, **16** and **19**, respectively. Quinones **27**, **29** and **30** were obtained from compounds **3** and **28** as previously described by us.

4.2.1. 9-Hydroxy-β-dunnione (*4*)

To a stirred solution of 5-hydroxydunniol (**32**, 25.5 mg, 0.1 mmol) in CH_2Cl_2 at −15 °C was added methanesulfonic acid (0.4 mL). After 3 min the reaction was quenched with water and extracted with CH_2Cl_2. The organic layer was dried over anhydrous Na_2SO_4, filtered, and evaporated under vacuum. Compound **4** was obtained as red crystals (25.5 mg, 100%); mp 144–146 °C; IR (KBr) 3450, 2956, 2929, 2870, 1693, 1644, 1602, 1466, 1303, 1259 cm^{-1}; ^1H NMR (500.13 MHz, $CDCl_3$): 7.87 (1H, s, OH), 7.62 (1H, dd, $J = 7.5$, 1.1 Hz, H-6), 7.37 (1H, dd, $J = 8.3$, 7.6 Hz, H-7), 7.11 (1H, dd, $J = 8.4$, 1.1 Hz, H-8), 4.72 (1H, q, $J = 6.7$ Hz, H-2), 1.46 (3H, d, $J = 6.7$ Hz, CH_3-10), 1.39 (3H, s, CH_3-11), 1.21 (3H, s, CH_3-12); ^{13}C NMR (125.77 MHz, $CDCl_3$): 181.0 (C-5), 175.4 (C-4), 167.7 (C-9b), 155.0 (C-9), 133.3 (C-7), 131.4 (C-5a), 124.6 (C-8), 123.3 (C-6), 122.6 (C-3a), 111.2 (C-9a), 94.6 (C-2), 43.2 (H-3), 25.5 (CH_3-11), 20.3 (CH_3-12), 14.7 (CH_3-10); HRMS found: 259.0975 $(M + H)^+$ calcd for $C_{15}H_{15}O_4$: 259.0965.

4.2.2. Hydroxy-α-dunnione (*37*)

A suspension of **4** (43 mg, 0.17 mmol) in 20% HCl (2.7 mL) was heated to 85 °C overnight. The reaction was quenched with water and extracted with CH_2Cl_2. The organic layer was dried

over anhydrous Na_2SO_4, filtered, and evaporated under vacuum. Compound **37** was obtained as orange crystals (43 mg, 100%); mp 105–106 °C; IR (KBr) 2963, 2923, 2850, 1680, 1633, 1602 cm^{-1}; ^1H NMR (500.13 MHz, $CDCl_3$): 12.40 (1H, d, $J = 0.4$ Hz, OH), 7.61 (1H, dd, $J = 7.4$, 1.2 Hz, H-8), 7.51 (1H, ddd, $J = 7.9$, 7.5, 0.5 Hz, H-7), 7.23 (1H, dd, $J = 8.4$, 1.2 Hz, H-6), 4.61 (1H, q, $J = 6.7$ Hz, H-2), 1.49 (3H, s, H-11), 1.45 (3H, d, $J = 6.7$ Hz, H-10), 1.30 (3H, s, H-12); ^{13}C NMR(125.77 MHz, $CDCl_3$): 188.7 (C-4), 177.9 (C-9), 161.3 (C-5), 159.4 (C-9a), 134.9 (C-7), 131.6 (C-8a), 130.5 (C-3a), 125.8 (C-6), 119.2 (C-8), 115.1 (C-4a), 92.1 (C-2), 45.0 (C-3), 25.8 (CH_3-11), 20.6 (CH_3-12), 14.2 (CH_3-10); HRMS found: 259.0972 $(M + H)^+$ calcd for $C_{15}H_{15}O_4$: 259.0965.

4.2.3. 9-Hydroxy-β-isodunnione (*6*)

To a stirred solution of **37** (43 mg, 0.17 mmol) in CH_2Cl_2 at −15 °C was added concentrated H_2SO_4 (0.8 mL) and stirring continued at room temperature overnight. The reaction mixture was cooled to 0 °C, diluted with water and extracted with CH_2Cl_2. The organic layer was dried over anhydrous Na_2SO_4, filtered, and evaporated under vacuum. The residue was purified by column chromatography on silica gel (hexane/EtOAc, gradient) to give **6** as dark red crystals (6.5 mg, 15%) and recovered **37** (32 mg, 74%); mp 75–76 °C; IR (KBr) 3440, 2973, 1642, 1604, 1257 cm^{-1}; ^1H NMR (500.13 MHz, $CDCl_3$): 7.87 (1H, d, $J = 0.5$ Hz, OH), 7.64 (1H, dd, $J = 7.5$, 1.1 Hz, H-6), 7.38 (1H, ddd, $J = 8.4$, 7.5, 0.3 Hz, H-7), 7.11 (1H, dd, $J = 8.5$, 1.1 Hz, H-8), 3.12 (1H, q, $J = 7.1$ Hz, H-3), 1.53 (3H, s, CH_3-10), 1.50 (3H, s, CH_3-11), 1.22 (3H, d, $J = 7.1$ Hz, CH_3-12); ^{13}C NMR (125.77 MHz, $CDCl_3$): 181.0 (C-5), 175.7 (C-4), 167.2 (C-9b), 155.1 (C-9), 133.4 (C-7), 131.4 (C-5a), 124.6 (C-8), 123.3 (C-6), 119.4 (C-3a), 111.3 (C-9a), 98.4 (C-2), 42.5 (C-3), 29.0 (C-10), 22.6 (C-11), 14.1 (C-12); HRMS found: 281.0786 $(M + Na)^+$ calcd for $C_{15}H_{14}NaO_4$: 281.0784.

4.2.4. 6-Hydroxy-β-dunnione (*5*)

Compound **5** (14.6 mg, 100%) was obtained as red crystals from compound **33** (14.6 mg, 0.06 mmol) and methanesulfonic acid (0.8 mL) following the procedure described for compound **4**; mp 151–152 °C (lit [54]. 151–152 °C); IR (KBr): 2958, 2916, 2848, 1733, 1640, 1615, 1592 cm^{-1}; ^1H NMR (500.13 MHz, $CDCl_3$): 11.93 (1H, s, OH), 7.53 (1H, dd, $J = 8.6$, 7.3 Hz, H-8), 7.19 (1H, dd, $J = 7.3$, 1.0 Hz, H-9), 7.10 (1H, dd, $J = 8.6$, 1.0 Hz, H-7), 4.65 (1H, q, $J = 6.7$ Hz, H-2), 1.46 (3H, d, $J = 6.7$ Hz, CH_3-10), 1.44 (3H, s, CH_3-11), 1.26 (3H, s, CH_3-12); ^{13}C NMR (125.77 MHz, $CDCl_3$): 185.5 (C-5), 174.9 (C-4), 167.7 (C-9b), 164.3 (C-6), 137.5 (C-8), 127.7 (C-9a), 123.3 (C-3a), 122.9 (C-7), 117.4 (C-9), 113.5 (C-5a), 92.8 (C-2), 44.1 (C-3), 25.7 (CH_3-11), 20.3 (CH_3-12), 14.5 (CH_3-10); HRMS found: 259.0972 $(M + H)^+$ calcd for $C_{15}H_{15}O_4$: 259.0965.

4.2.5. 8-Hydroxy-α-dunnione (*38*)

A solution of **5** (17.1 mg, 0.07 mmol) in concentrated HCl (3.2 mL) was heated at 85 °C overnight. The reaction was quenched with water and extracted with CH_2Cl_2. The organic layer was dried over anhydrous Na_2SO_4, filtered, and evaporated under vacuum. The residue was purified by column chromatography on silica gel (hexane/EtOAc, gradient) to give **38** as yellow crystals (8.5 mg, 50%) and **5** (6.7 mg, 39%) was recovered unreacted; mp 117–118 °C; IR (KBr): 2964, 2926, 1645, 1609 cm^{-1}; ^1H NMR (500.13 MHz, $CDCl_3$): 11.66 (1H, s, OH), 7.58 (2H, m, H-5 y 6), 7.19 (1H, m, H-7), 4.60 (1H, q, $J = 6.6$ Hz, H-2), 1.47 (3H, s, CH_3-11), 1.45 (3H, d, $J = 6.7$ Hz, CH_3-10), 1.28 (3H, s, CH_3-12); ^{13}C NMR(125.77 MHz, $CDCl_3$): 183.3 (C-9), 181.5 (C-4), 161.8 (C-8), 158.4 (C-9a), 136.9 (C-6), 133.7 (C-4a), 131.8 (C-3a), 123.8 (C-7), 118.9 (C-5), 114.6 (C-8a), 91.9 (C-2), 45.2 (C-3), 25.7 (CH_3-11), 20.5 (CH_3-12), 14.2 (CH_3-10); HRMS found: 259.0972 $(M + H)^+$ calcd for $C_{15}H_{15}O_4$: 259.0965.

4.2.6. 6-Hydroxy-β-isodunnione (*7*)

A solution of **38** (6.0 mg, 0.02 mmol) in concentrated H_2SO_4 (0.6 mL) was stirred at room temperature overnight. The reaction was cooled to 0 °C, quenched with water and extracted with CH_2Cl_2. The organic layer was dried over anhydrous Na_2SO_4, filtered, and evaporated under vacuum. The residue was purified by column chromatography on silica gel (hexane/EtOAc, gradient) to give **7** as red crystals (1.9 mg, 32%) and **38** (3.3 mg, 55%) was recovered unreacted; mp 117–118 °C (lit. [55] 116–117 °C); IR (KBr): 2918, 2845, 1735, 1648, 1615, 1592 cm^{-1}; ^1H NMR (500.13 MHz, $CDCl_3$): 11.94 (1H, s, OH), 7.52 (1H, dd, $J = 8.5$, 7.4 Hz, H-8), 7.18 (1H, dd, $J = 7.3$, 1.0 Hz, H-9), 7.11 (1H, dd, $J = 8.6$, 1.0 Hz, H-7), 3.20 (1H, q, $J = 7.1$ Hz, H-3), 1.51 (3H, s, CH_3-10), 1.49 (3H, s, CH_3-11), 1.27 (3H, d, $J = 7.1$ Hz, CH_3-12); ^{13}C NMR (125.77 MHz, $CDCl_3$): 185.7 (C-5), 175.2 (C-4), 167.3 (C-9b), 164.3 (C-6), 137.5 (C-8), 127.9 (C-9a), 123.0 (C-7), 119.9 (C-3a), 117.5 (C-9), 113.6 (C-5a), 95.4 (C-2), 43.5 (C-3), 28.9 (CH_3-10), 22.4 (CH_3-11), 14.1 (CH_3-12); HRMS found: 281.0794 $(M + Na)^+$ calcd for $C_{15}H_{14}NaO_4$: 281.0784.

4.2.7. 5-Hydroxylomatiol (*39*)

A suspension of 5-hydroxylapachol (**14**, 50 mg, 0.2 mmol) and zinc dust (100 mg) in acetic anhydride (1 mL) and triethylamine (10 μL) was stirred at room temperature for 1.5 h. The solution was filtered and the filtrate was diluted with water and extracted with CH_2Cl_2. The organic layer was dried over anhydrous Na_2SO_4, filtered, and evaporated under vacuum to give a pale yellow oil (47.6 mg). This oil was dissolved in a mixture of acetic anhydride (2.9 mL) and glacial acetic acid (1.8 mL) and selenium dioxide (9 mg) added. The mixture was heated under reflux for 1 h, cooled and diluted with water. The resulting oil was extracted with diethyl ether, washed successively with water and 2% sodium hydroxide, dried over anhydrous Na_2SO_4, filtered and concentrated. The residual viscous oil (82.3 mg) was dissolved in methanol (3.2 mL) and treated with 6 M KOH (3.2 mL), and the solution was heated under reflux for 15 min. After cooling the mixture was carefully acidified with HCl 5% and extracted with diethyl ether. The organic layer was washed with water, dried over anhydrous Na_2SO_4, filtered, and evaporated under vacuum. The residue was purified by column chromatography on silica gel (hexane/EtOAc, gradient) to give **39** as yellow crystals (10.1 mg, 19%); mp 166–167 °C; IR (KBr): 3339, 3224, 2956, 2926, 2850, 1735, 1645, 1620, 1472, 1467 cm^{-1}; ^1H NMR (500.13 MHz, $CDCl_3$): 12.48 (1H, s, OH-5), 7.61 (1H, dd, $J = 7.4$, 1.0 Hz, H-8), 7.54 (1H, t, $J = 7.9$ Hz, H-7), 7.27 (1H, dd, $J = 8.3$, 0.9 Hz, H-6), 5.48 (1H, dt, $J = 7.3$, 1.2 Hz, H-2′), 3.97 (2H, s, H-4′), 3.34 (2H, d, $J = 7.3$ Hz, H-1′), 1.83 (3H, s, CH_3); ^{13}C NMR(125.77 MHz, $CDCl_3$): 190.6 (C-4), 180.9 (C-1), 160.8 (C-5), 154.4 (C-2), 136.7 (C-3′), 134.8 (C-7), 129.7 (C-8a), 125.7 (C-6), 122.6 (C-3), 120.7 (C-2′), 119.0 (C-8), 114.3 (C-4a), 68.1 (C-4′), 21.4 (C-1′), 13.6 (C-5′); HRMS found: 297.0742 $(M + Na)^+$ calcd for $C_{15}H_{14}NaO_5$: 297.0733.

4.2.8. 8-Hydroxylomatiol (*40*)

Compound **40** (21.4 mg, 49%) was obtained as yellow crystals from 8-hydroxylapachol (**15**, 42 mg, 0.16 mmol) following the procedure described for compound **39**; mp 104–105 °C; IR (KBr): 3386, 2920, 2848, 1714, 1626, 1452 cm^{-1}; ^1H NMR (500.13 MHz, $CDCl_3$): 11.09 (1H, s, OH-8), 7.64 (2H, m, H-5 and H-6), 7.20 (1H, dd, $J = 7.7$, 1.9 Hz, H-7), 5.48 (1H, tsep, $J = 7.2$, 1.5 Hz, H-2′), 4.00 (2H, s, H-4′), 3.36 (2H, dd, $J = 7.0$, 0.4 Hz, H-1′), 1.84 (3H, s, CH_3); ^{13}C NMR(125.77 MHz, $CDCl_3$): 184.8 (C-1), 183.6 (C-4), 161.2 (C-8), 152.6 (C-2), 137.7 (C-5 o 6), 137.0 (C-3′), 132.6 (C-4a), 123.9 (C-3), 123.2 (C-7), 120.7 (C-2′), 119.7 (C-5 o 6), 112.9 (C-8a), 68.6 (C-4′), 22.2 (C-1′), 13.8 (C-5′); HRMS found: 297.0738 $(M + Na)^+$ calcd for $C_{15}H_{14}NaO_5$: 297.0733.

4.2.9. 9-Hydroxy-dehydro-iso-β-lapachone (**8**)

5-Hydroxylomatiol (**39**, 6.2 mg, 0.02 mmol) was treated at 0 °C with a mixture of H_2SO_4–H_2O (5:3) (1 mL). The mixture was stirred until the 5-hydroxylomatiol was completely dissolved and the solution was then immediately poured into water and extracted with CH_2Cl_2. The organic layer was dried over anhydrous Na_2SO_4, filtered, and evaporated under vacuum. The residue was purified by column chromatography on silica gel (hexane/EtOAc, gradient) to give **8** as violet crystals (2.6 mg, 50%); mp 120–121 °C; IR (KBr) 3157, 2962, 2921, 1628, 1594, 1543, 1260 cm^{-1}; ^1H NMR (500.13 MHz, $CDCl_3$): 7.88 (1H, s, OH), 7.74 (1H, dd, $J = 7.5$, 1.1 Hz, H-6), 7.49 (1H, dd, $J = 8.3$, 7.5 Hz, H-7), 7.21 (1H, dd, $J = 8.5$, 1.1 Hz, H-8), 5.62 (1H, dd, $J = 10.2$, 7.8 Hz, H-2), 5.17 (1H, d, $J = 0.9$ Hz, H-11a), 5.09 (1H, dd, $J = 1.3$, 1.1 Hz, H-11b), 3.28 (1H, dd, $J = 15.4$, 10.4 Hz, H-3a), 2.95 (1H, dd, $J = 15.4$, 7.8 Hz, H-3b), 1.83 (3H, dd, $J = 1.3$, 0.9 Hz, CH_3); ^{13}C NMR(125.77 MHz, $CDCl_3$): 180.6 (C-5), 175.3 (C-4), 169.0 (C-9b), 154.9 (C-9), 141.0 (C-10), 133.7 (C-7), 131.3 (C-5a), 124.8 (C-8), 123.7 (C-6), 115.1 (C-11), 114.5 (C-3a), 110.9 (C-9a), 92.0 (C-2), 30.0 (C-3), 16.7 (CH_3); HRMS found: 257.0800 $(M + H)^+$ calcd for $C_{15}H_{13}O_4$: 257.0808.

4.2.10. 6-Hydroxy-dehydro-iso-β-lapachone (**9**)

Compound **9** (11 mg, 54%) was obtained as red crystals from 8-hydroxylomatiol (**40**, 21.4 mg, 0.08 mmol) following the procedure described for compound **8**; mp 150 °C; IR (KBr) 2930, 1645, 1615, 1581 cm^{-1}; ^1H NMR (500.13 MHz, $CDCl_3$): 11.94 (1H,d, $J = 0.3$, OH), 7.55 (1H, dd, $J = 8.4$, 7.3 Hz, H-8), 7.24 (1H, dd, $J = 7.3$, 1.0 Hz, H-9), 7.14 (1H, dd, $J = 8.7$, 1.0 Hz, H-7), 5.47 (1H, dd, $J = 10.5$, 7.8 Hz, H-2), 5.13 (1H, d, $J = 0.9$ Hz, H-11a), 5.03 (1H, t, $J = 1.3$ Hz, H-11b), 3.29 (1H, dd, $J = 15.6$, 10.5 Hz, H-3a), 2.95 (1H, dd, $J = 15.6$, 7.8 Hz, H-3b), 1.80 (3H, t, $J = 1.0$ Hz, CH_3); ^{13}C NMR(125.77 MHz, $CDCl_3$): 185.2 (C-5), 174.9 (C-4), 169.2 (C-9b), 164.5 (C-6), 141.8 (C-10), 137.7 (C-8), 127.1 (C-9a), 123.4 (C-7), 117.5 (C-9), 115.2 (C-3a), 113.9 (C-11), 113.4 (C-5a), 89.8 (C-2), 31.1 (C-3), 16.8 (CH_3); HRMS found: 257.0809 $(M + H)^+$ calcd. for $C_{15}H_{13}O_4$: 257.0808.

4.3. Molecular descriptors calculation

The compounds were first drawn with HyperChem for Windows [56], and then the .hin files were converted into .sdf by using the Open Babel 2.3.1 software [57]. A set of 931 conformation-independent molecular descriptors were computed using E-Dragon [58]. This useful and well-known descriptors database included thirteen descriptor families: Constitutional, Topological, Walk and Path Count, Connectivity Index, Information Index, Edge Adjacency Index, Topological Charge Index, Burden Eigenvalues, Eigenvalue-Based Index, 2D-Autocorrelation, Functional Group Count, Atom-Centred Fragment, and Molecular Property [51].

In addition, atomic charge density-based descriptors were obtained, encoding electronic and structural information relevant to the chemistry of intermolecular interactions, by means of Recon 5.5 [59]. This sort of descriptors were not provided by E-Dragon, while the robustness of Recon had previously been demonstrated elsewhere [60,61]. Recon was an algorithm for the reconstruction of molecular charge densities and charge density-based electronic properties of molecules, using atomic charge density fragments precomputed from ab initio wavefunctions. The method was based on the Quantum Theory of Atoms in Molecules [62]. A library of atomic charge density fragments had been built in a form that allows for the rapid retrieval of the fragments and molecular assembly. The .sdf molecular format was employed as input for the generation of 248 Transferable Atom Equivalent (TAE) descriptors developed by Breneman et al. [63]. In this way, the total number of calculated molecular descriptors was of 1179 variables.

4.4. Biology

All starting materials were commercially available research-grade chemicals and used without further purification. RPMI 1640 medium was purchased from Flow Laboratories (Irvine, UK), fetal calf serum (FCS) was from Gibco (Grand Island, NY), trichloroacetic acid (TCA) and glutamine were from Merck (Darmstadt, Germany), and penicillin G, streptomycin, DMSO and sulforhodamine B (SRB) were from Sigma (St Louis, MO).

4.4.1. Cells, culture and plating

The human solid tumor cell lines HBL-100, HeLa, SW1573, and WiDr were used in this study. These cell lines were a kind gift from Prof. G.J. Peters (VU Medical Center, Amsterdam, The Netherlands). Cells were maintained in 25 cm^2 culture flasks in RPMI 1640 supplemented with 5% heat inactivated fetal calf serum and 2 mM L-glutamine in a 37 °C, 5% CO_2, 95% humidified air incubator. Exponentially growing cells were trypsinized and resuspended in antibiotic containing medium (100 units penicillin G and 0.1 mg of streptomycin per mL). Single cell suspensions displaying >97% viability by trypan blue dye exclusion were subsequently counted. After counting, dilutions were made to give the appropriate cell densities for inoculation onto 96-well microtiter plates. Cells were inoculated in a volume of 100 μL per well at densities 10,000 (SW1573 and HBL-100) of 15,000 (HeLa), and 20,000 (WiDr) cells per well, based on their doubling times.

Acknowledgments

We thank the financial support provided by the National Research Council of Argentina (CONICET) PIP11220100100151 and PIP11220100100447 projects and to Ministerio de Ciencia, Tecnología e Innovación Productiva for the electronic library facilities. Co-financed by the EU Research Potential (FP7-REGPOT-2012-CT2012-31637-IMBRAIN), the European Regional Development Fund (FEDER), and the Spanish Instituto de Salud Carlos III (PI11/00840).

Appendix A. Supplementary data

Supplementary data related to this article can be found at http://dx.doi.org/10.1016/j.ejmech.2014.02.057.

References

[1] G. Powis, Free radical formation by antitumor quinones, Free Radical Biology & Medicine 6 (1989) 63–101.
[2] C. Asche, Antitumour quinones, Mini-Reviews in Medicinal Chemistry 5 (2005) 449–467.
[3] L. Constantino, D. Barlocco, Privileged structures as leads in medicinal chemistry, Current Medicinal Chemistry 13 (2006) 65–85.
[4] J. Li, K.K.-C. Liu, S. Sakya, Synthetic approaches to the 2004 new drugs, Mini-Reviews in Medicinal Chemistry 5 (2005) 1133–1144.
[5] R.W. De Simone, K.S. Currie, S.A. Mitchell, J.W. Darrow, D.A. Pippin, A, Privileged structures: applications in drug discovery, Combinatorial Chemistry & High Throughput Screening 7 (2004) 473–494.
[6] K.O. Eyong, G.N. Folefoc, V. Kuete, V.P. Beng, K. Krohn, H. Hussain, A.E. Nkengfack, M. Saeftel, S.R. Sarite, A. Hoerauf, Newbouldiaquinone A: a naphthoquinone-anthraquinone ether coupled pigment, as a potential antimicrobial and antimalarial agent from *Newbouldia laevis*, Phytochemistry 67 (2006) 605–609.
[7] V. Kuete, K.O. Eyong, G.N. Folefoc, V.P. Beng, H. Hussain, K. Krohn, A.E. Nkengfack, Antimicrobial activity of the methanolic extract and of the chemical constituents isolated from *Newbouldia laevis*, Die Pharmazie 62 (2007) 552–556.
[8] J. Breger, B.B. Fuchs, G. Aperis, T.I. Moy, F.M. Ausubel, E. Mylonakis, Antifungal chemical compounds identified using a *C. elegans* pathogenicity assay, PLoS Pathogens 3 (2007) 168–178.
[9] A. Portillo, R. Vila, B. Freixa, T. Adzet, S. Cañigueral, Antifungal activity of Paraguayan plants used in traditional medicine, Journal of Ethnopharmacology 76 (2001) 93–98.

[10] A.V. Pinto, S.L. De Castro, The trypanocidal activity of naphthoquinones: a review, Molecules 14 (2009) 4570–4590.
[11] H. Hussain, K. Krohn, V.U. Ahmad, G.A. Miana, I.R. Green, Lapachol: an overview, Arkivoc 2 (2007) 145–171.
[12] X. Cheng, F. Liu, T. Yan, X. Zhou, L. Wu, K. Liao, G. Wang, Metabolic profile, enzyme kinetics, and reaction phenotyping of β-lapachone metabolism in human liver and intestine in vitro, Molecular Pharmaceutics 9 (2012) 3476–3485.
[13] R.J. Boorstein, A.B. Pardee, β-Lapachone greatly enhances MMS lethality to human fibroblasts, Biochemical and Biophysical Research Communications 118 (1984) 828–834.
[14] P.S. Guin, S. Das, P.C. Mandal, Electrochemical reduction of quinones in different media: a review, International Journal of Electrochemical Science 2011 (2011) 1–22.
[15] H.-X. Chang, T.-C. Chou, N. Savaraj, L.F. Liu, C. Yu, C.C. Cheng, Design of antineoplastic agents based on the "2-phenylnaphthalene-type" structural pattern. 4. Synthesis and biological activity of 2-chloro-3-(substituted phenoxy)-1,4-naphthoquinones and related 5,8-dihydroxy-1,4-naphthoquinones, Journal of Medicinal Chemistry 42 (1999) 405–408.
[16] K.-I. Hayashi, F.-R. Chang, Y. Nakanishi, K.F. Bastow, G. Cragg, A.T. Mc Phail, H. Nozaki, K.-H. Lee, Antitumor Agents. 233 lantalucratins A-F, new cytotoxic naphthoquinones from *Lantana involucrata*, Journal of Natural Products 67 (2004) 990–993.
[17] R.M. Khan, S.M. Mlungwana, 5-Hydroxylapachol: a cytotoxic agent from *Tectona grandis*, Phythochemistry 50 (1999) 439–442.
[18] M. Yamashita, M. Kaneko, H. Tokuda, K. Nishimura, Y. Kumeda, A. Iida, Synthesis and evaluation of bioactive naphthoquinones from the Brazilian medicinal plant, *Tabebuia avellanedae*, Bioorganic & Medicinal Chemistry 17 (2009) 6286–6291.
[19] E.L. Bonifazi, C. Rios-Luci, L.G. León, G. Burton, J.M. Padrón, R.I. Misico, Antiproliferative activity of synthetic naphthoquinones related to lapachol. First synthesis of 5-hydroxylapachol, Bioorganic & Medicinal Chemistry 18 (2010) 2621–2630.
[20] C. Rios-Luci, E.L. Bonifazi, L.G. León, J.C. Montero, G. Burton, A. Pandiella, R.I. Misico, J.M. Padrón, β-Lapachone analogs with enhanced antiproliferative activity, European Journal of Medicinal Chemistry 53 (2012) 264–274.
[21] C. Hansch, A. Leo, Exploring QSAR, in: Fundamentals and Applications in Chemistry and Biology, American Chemical Society, Washington, D. C., 1995.
[22] H. Kubinyi, QSAR: Hansch Analysis and Related Approaches, Wiley-Interscience, New York, 2008.
[23] T. Puzyn, J. Leszczynski, M.T.D. Cronin (Eds.), Recent Advances in QSAR Studies: Methods and Applications, Springer Science&Business Media B.V., Netherlands, 2010.
[24] S.G. Renou, S.E. Asís, M.I. Abasolo, D.G. Bekerman, A.M. Bruno, Monoarylhydrazones of α-lapachone: synthesis, chemical properties and antineoplastic activity, Die Pharmazie 58 (2003) 690–695.
[25] R.P. Verma, C. Hansch, Elucidation of structure-activity relationships for 2- or 6-substituted-5,8-dimethoxy-1,4-naphthoquinones, Bioorganic & Medicinal Chemistry 12 (2004) 5997–6009.
[26] R.P. Verma, Understanding topoisomerase I and II in terms of QSAR, Bioorganic & Medicinal Chemistry 13 (2005) 1059–1067.
[27] B. Kumar, Quantitative structure activity relationship (QSAR) modeling of 2-X-5,8-dimethoxy-1,4-naphthoquinones against L1210 cells, International Journal of Pharmacy and Pharmaceutical Sciences 4 (2012) 445–448.
[28] L. Saíz-Urra, M.P. González, M. Teijeira, 2D-autocorrelation descriptors for predicting cytotoxicity of naphthoquinone ester derivatives against oral human epidermoid carcinoma, Bioorganic & Medicinal Chemistry 15 (2007) 3565–3571.
[29] A. Takano, K. Hashimoto, M. Ogawa, J. Koyanagi, T. Kurihara, H. Wakabayashi, H. Kikuchi, Y. Nakamura, N. Motohashi, H. Sakagami, K. Yamamoto, A. Tanaka, Tumor-specific cytotoxicity and type of cell death induced by naphtho[2,3-b]furan-4,9-diones and related compounds in human tumor cell lines: relationship to electronic structure, Anticancer Research 29 (2009) 455–464.
[30] A. Bargiotti, L. Musso, S. Dallavalle, L. Merlini, G. Gallo, A. Ciacci, G. Giannini, W. Cabri, S. Penco, L. Vesci, M. Castorina, F.M. Milazzo, M.L. Cervoni, M. Barbarino, C. Pisano, C. Giommarelli, V. Zuco, M. De Cesare, F. Zunino, Isoxazolo(aza)naphthoquinones: a new class of cytotoxic Hsp90 inhibitors, European Journal of Medicinal Chemistry 53 (2012) 64–75.
[31] Y. Ma, J.-G. Wang, B. Wang, Z.-M. Li, Integrating molecular docking, DFT and CoMFA/CoMSIA approaches for a series of naphthoquinone fused cyclic α-aminophosphonates that act as novel topoisomerase II inhibitors, Journal of Molecular Modeling 17 (2011) 1899–1909.
[32] E. Pérez-Sacau, R.G. Díaz-Peñate, A. Estévez-Braun, A.G. Ravelo, J.M. García-Castellano, L. Pardo, M. Campillo, Synthesis and pharmacophore modeling of naphthoquinone derivatives with cytotoxic activity in human promyelocytic leukemia HL-60 cell line, Journal of Medicinal Chemistry 50 (2007) 696–706.
[33] J. Verma, V.M. Khedkar, E.C. Coutinho, 3D-QSAR in drug design – a review, Current Topics in Medicinal Chemistry 10 (2010) 95–115.
[34] P.R. Duchowicz, N.C. Comelli, E.V. Ortiz, E.A. Castro, QSAR study for carcinogenicity in a large set of organic compounds, Current Drug Safety 7 (2012) 282–288.
[35] P.O. Miranda, J.M. Padrón, J.I. Padrón, J. Villar, V.S. Martín, Prins-type synthesis and SAR study of cytotoxic alkyl chloro dihydropyrans, ChemMedChem 1 (2006) 323–329.
[36] P.R. Duchowicz, E.A. Castro, F.M. Fernández, Alternative algorithm for the search of an optimal set of descriptors in QSAR-QSPR studies, MATCH: Communications in Mathematical and in Computer Chemistry 55 (2006) 179–192.
[37] P.R. Duchowicz, E.A. Castro, F.M. Fernández, M.P. González, A new search algorithm of QSPR/QSAR theories: normal boiling points of some organic molecules, Chemical Physics Letters 412 (2005) 376–380.
[38] P.R. Duchowicz, A. Talevi, L.E. Bruno-Blanch, E.A. Castro, New QSPR study for the prediction of aqueous solubility of drug-like compounds, Bioorganic & Medicinal Chemistry Letters 16 (2008) 7944–7955.
[39] M. Goodarzi, P.R. Duchowicz, C.H. Wu, F.M. Fernández, E.A. Castro, New hybrid genetic based support VECTOR regression as QSAR approach for analyzing flavonoids-GABA(A) complexes, Journal of Chemical Information and Modeling 49 (2009) 1475–1485.
[40] A.B. Pomilio, M.A. Giraudo, P.R. Duchowicz, E.A. Castro, QSPR analyses for aminograms in food: citrus juices and concentrates, Food Chemistry 123 (2010) 917–927.
[41] A. Talevi, M. Goodarzi, E.V. Ortiz, P.R. Duchowicz, C.L. Bellera, G. Pesce, E.A. Castro, L.E. Bruno-Blanch, Prediction of drug intestinal absorption by new linear and non-linear QSPR, European Journal of Medicinal Chemistry 46 (2011) 218–228.
[42] G. Pasquale, G.P. Romanelli, J.C. Autino, J. García, E.V. Ortiz, P.R. Duchowicz, Quantitative structure-activity relationships on chalcone derivatives: mosquito larvicidal studies, Journal of Agricultural and Food Chemistry 60 (2012) 692–697.
[43] A.G. Mercader, P.R. Duchowicz, F.M. Fernández, E.A. Castro, Replacement method and enhanced replacement method versus the genetic algorithm approach for the selection of molecular descriptors in QSPR/QSAR theories, Journal of Chemical Information and Modeling 50 (2010) 1542–1548.
[44] A.G. Mercader, P.R. Duchowicz, F.M. Fernández, E.A. Castro, Advances in the replacement and enhanced replacement method in QSAR and QSPR theories, Journal of Chemical Information and Modeling 51 (2011) 1575–1581.
[45] Matlab, Matlab 7.0, The MathWorks, Inc., Masachussetts, USA, http://www.mathworks.com.
[46] A. Golbraikh, A. Tropsha, Beware of q2!, Journal of Molecular Graphics and Modelling 20 (2002) 269–276.
[47] S. Wold, L. Eriksson, Statistical validation of QSAR results, in: H. van de Waterbeemd (Ed.), Chemometrics Methods in Molecular Design, VCH, Weinheim, 1995, pp. 309–318.
[48] P. Gramatica, Principles of QSAR models validation: internal and external, QSAR & Combinatorial Science 26 (2007) 694–701.
[49] L. Eriksson, J. Jaworska, A.P. Worth, M.T. Cronin, R.M. McDowell, P. Gramatica, Methods for reliability and uncertainty assessment and for applicability evaluations of classification- and regression-based QSARs, Environmental Health Perspectives 111 (2003) 1361–1375.
[50] N.R. Draper, H. Smith, Applied Regression Analysis, 1981. New York.
[51] R. Todeschini, V. Consonni, Molecular Descriptors for Chemoinformatics (Methods and Principles in Medicinal Chemistry), Wiley-VCH, Weinheim, 2009.
[52] A.G. Ravelo, A. Estévez-Braun, E. Pérez-Sacau, The chemistry and biology of lapachol and related natural products: α- and β-lapachones, Studies in Natural Products Chemistry 29 (2003) 719–760.
[53] S.C. Hooker, The constitution of lapachol and its derivatives. Part V. The structure of Paternò's "isolapachone, Journal of the American Chemical Society 58 (1936) 1190–1197.
[54] K. Inoue, S. Ueda, H. Nayeshiro, H. Inouye, Structures of unusually prenylated naphthoquinones of *Streptocarpus dunii* and its cell cultures, Chemical and Pharmaceutical Bulletin 30 (1982) 2265–2268.
[55] V. Guay, P. Brassard, Synthesis of (±)-7- and 8-Hydroxydunnione, Journal of Natural Products 49 (1986) 122–125.
[56] HyperChem 7, Hypercube, Inc., http://www.hyper.com.
[57] OpenBabel 2.3.1, OpenBabel 2.3.1, http://openbabel.org/wiki/Windows_GUI.
[58] E-Dragon, Milano Chemometrics and QSAR Research Group, VCCLAB, Virtual Computational Chemistry Laboratory, 2005. http://michem.disat.unimib.it/chm.
[59] Recon, Recon, Rensselaer Polytechnic Institute, Troy, New York, USA, 2002. http://www.drugmining.com.
[60] B.K. Lavine, C.E. Davidson, C. Breneman, W. Katt, Electronic Van der Waals SURFACE property descriptors and genetic algorithms for developing structure-activity correlations in olfactory databases, Journal of Chemical Information and Modeling 43 (2003) 1890–1905.
[61] A. Worachartcheewan, C. Nantasenamat, T. Naenna, C. Isarankura-Na-Ayudhya, V. Prachayasittikul, Modeling the activity of furin inhibitors using artificial neural network, European Journal of Medicinal Chemistry 44 (2009) 1664–1673.
[62] R.F.W. Bader, Atoms in Molecules-a Quantum Theory, 1990. U.K.
[63] C.M. Breneman, L.W. Weber, Transferable atom equivalents. Assembling accurate electrostatic potential fields for large molecules from ab initio and PROAIMS results on model systems, in: G.A. Jeffrey, J.F. Piniella (Eds.), The Application of Charge Density Research to Chemistry and Drug Design, 1991. New York.